JOURNAL OF AGRICULTURAL AND FOOD CHEMISTRY

Agricultural and Environmental Chemistry

Synthesis, Antiviral Activity and Induction of Plant Resistance of Indole Analogues Bearing Dithioacetal Moiety

Baoan Song, Chunle Wei, Jian Zhang, Jing Shi, Xiuhai Gan, and De-Yu Hu

J. Agric. Food Chem., **Just Accepted Manuscript** • DOI: 10.1021/acs.jafc.9b05357 • Publication Date (Web): 13 Nov 2019

is published by the American Chemical Society. 1155 Sixteenth Street N.W., Washington, DC 20036

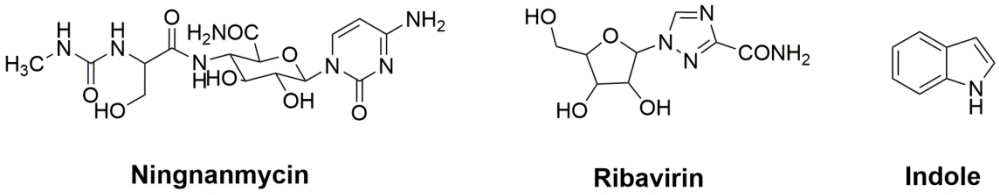

Figure 1. Chemical structures of Ningnanmycin, Ribavirin, and Indole.

162x32mm (300 x 300 DPI)

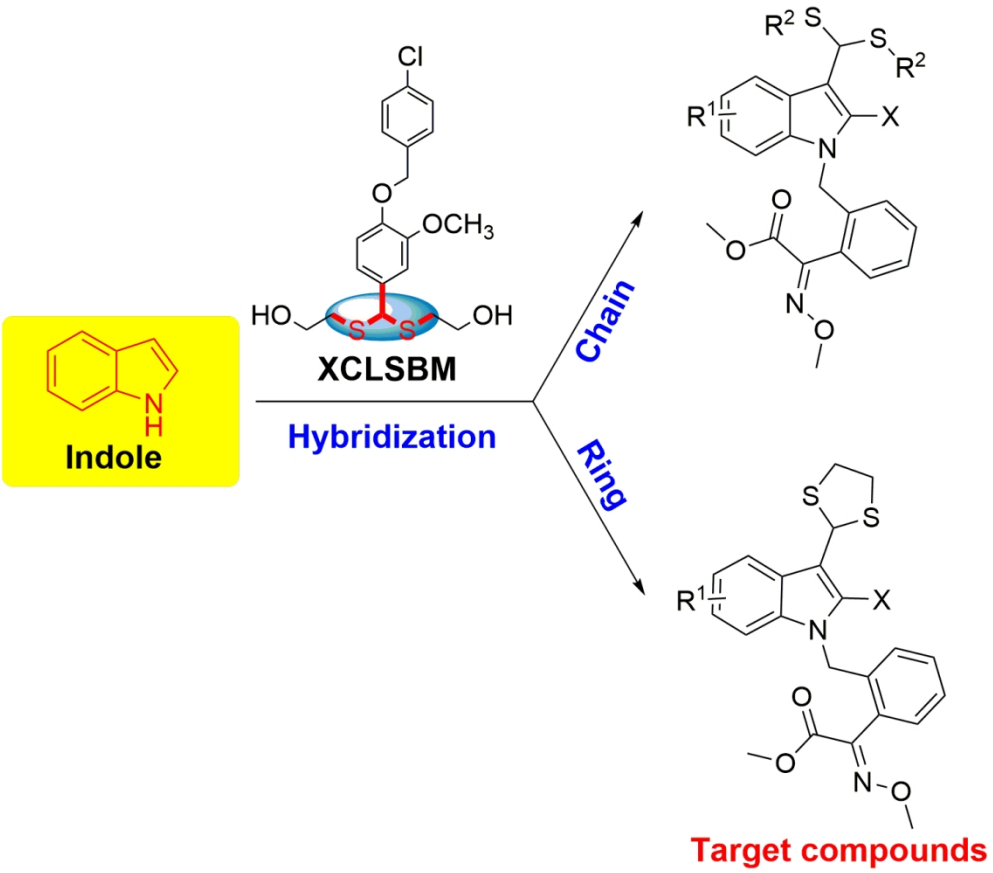

Figure 2. Design of target compounds.

127x112mm (300 x 300 DPI)

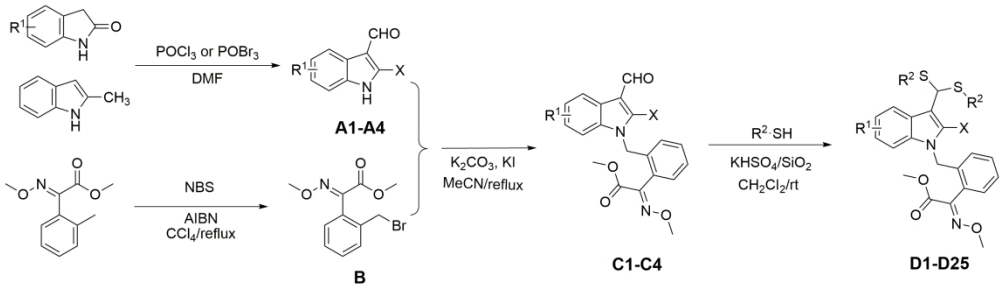

A1: R^1=H, X=Cl
A2: R^1=H, X=Br
A3: R^1=5-Br, X=Cl
A4: R^1=H, X=CH_3
C1: R^1=H, X=Cl
C2: R^1=H, X=Br
C3: R^1=5-Br, X=Cl
C4: R^1=H, X=CH_3

D1: R^1=H, R^2=2-Hydroxyethyl, X=Cl
D2: R^1=H, R^2=Ethyl, X=Cl
D3: R^1=H, R^2=Propyl, X=Cl
D4: R^1=H, R^2=Isopropyl, X=Cl
D5: R^1=H, R^2=4-chlorophenyl, X=Cl
D6: R^1=H, R^2=2,4-dichlorophenyl, X=Cl
D7: R^1=H, R^2=Butyl, X=Cl
D8: R^1=H, R^2=Tert-butyl, X=Cl
D9: R^1=H, R^2=Dodecyl, X=Cl
D10: R^1=H, R^2=2-Hydroxyethyl, X=Br
D11: R^1=H, R^2=Ethyl, X=Br
D12: R^1=H, R^2=Propyl, X=Br

D13: R^1=H, R^2=Isopropyl, X=Br
D14: R^1=H, R^2=4-chlorophenyl, X=Br
D15: R^1=H, R^2=2,4-dichlorophenyl, X=Br
D16: R^1=H, R^2=Butyl, X=Br
D17: R^1=H, R^2=Tert-butyl, X=Br
D18: R^1=H, R^2=Dodecyl, X=Br
D19: R^1=5-Br, R^2=2-Hydroxyethyl, X=Cl
D20: R^1=5-Br, R^2=4-chlorophenyl, X=Cl
D21: R^1=5-Br, R^2=Propyl, X=Cl
D22: R^1=H, R^2=2-Hydroxyethyl, X=CH_3
D23: R^1=H, R^2=Ethyl, X=CH_3
D24: R^1=H, R^2=Propyl, X=CH_3
D25: R^1=H, R^2=4-chlorophenyl, X=CH_3

Figure 3. Synthetic route for target compounds D1-D25.

243x140mm (300 x 300 DPI)

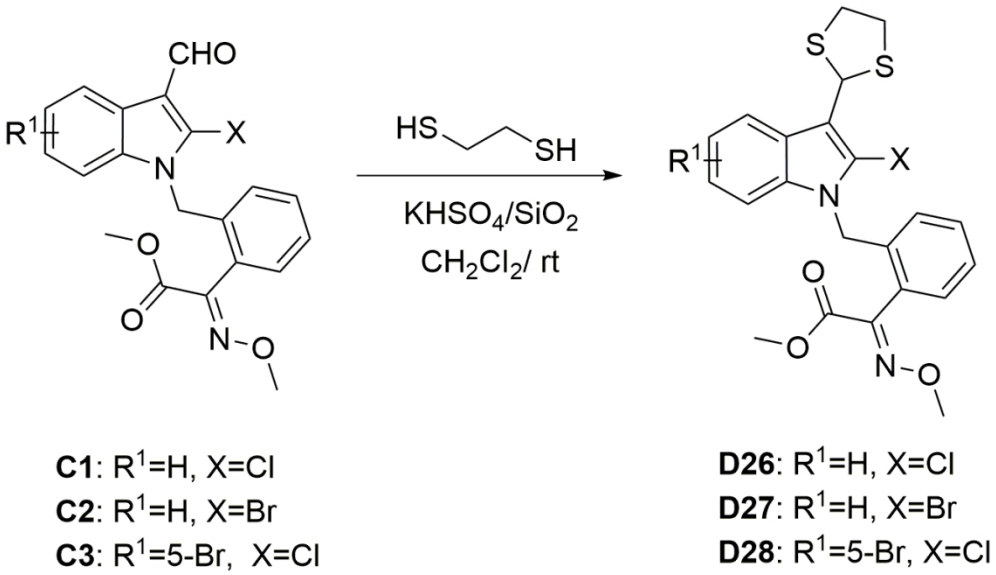

Figure 4. Synthetic route for target compounds D26-D28.

113x65mm (300 x 300 DPI)

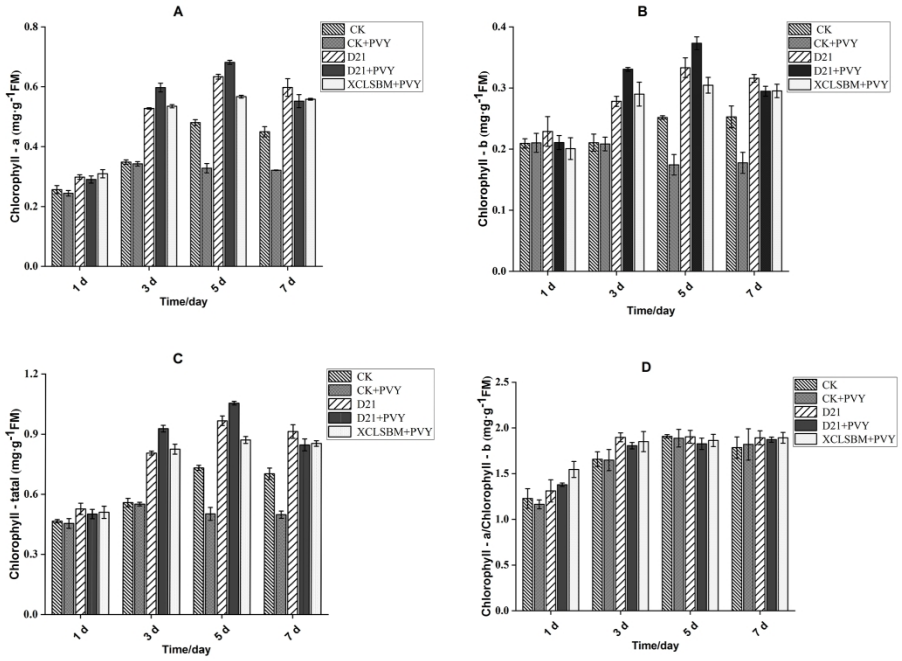

Figure 5. Effects of compound D21 on chlorophyll a (A), chlorophyll b (B) and chlorophyll total (C), chlorophyll a/b (D) in tobacco leaves. Straight bars signify mean ± SD (n = 3).

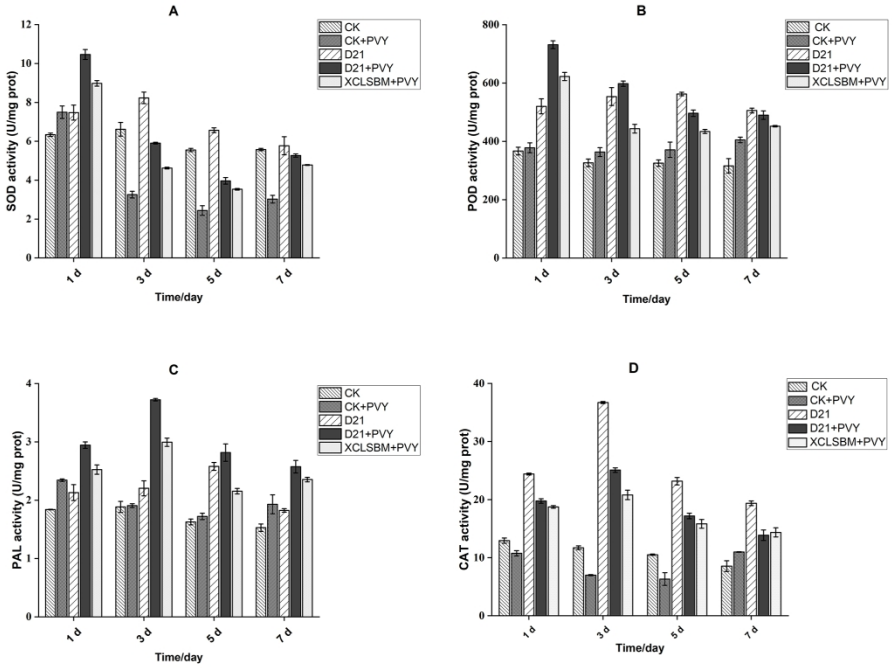

Figure 6. Effects of compound D21 on superoxide dismutase (SOD, A), peroxidase (POD, B), phenylalanine ammonia lyase (PAL, C), and catalase (CAT, D) activity in tobacco leaves. Straight bars signify mean ± SD (n= 3).

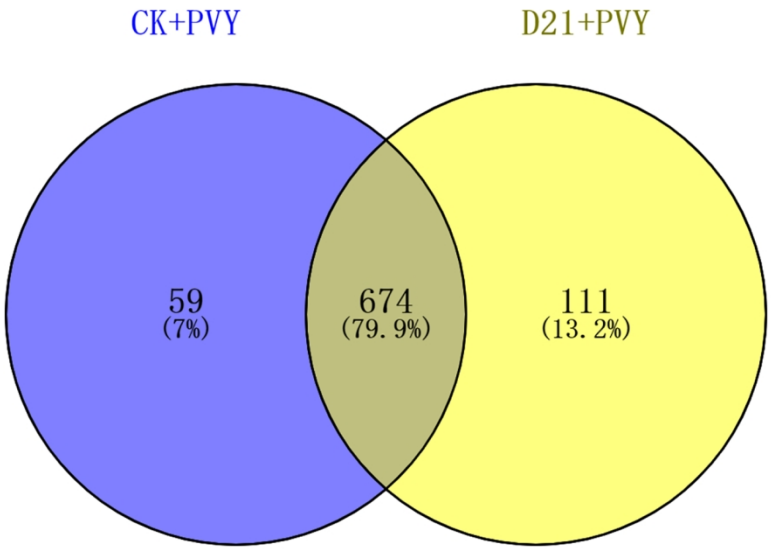

Figure 7. Venn diagram shows that the proteome distribution between the D21+PVY and CK+PVY groups changes uniquely and shares proteins.

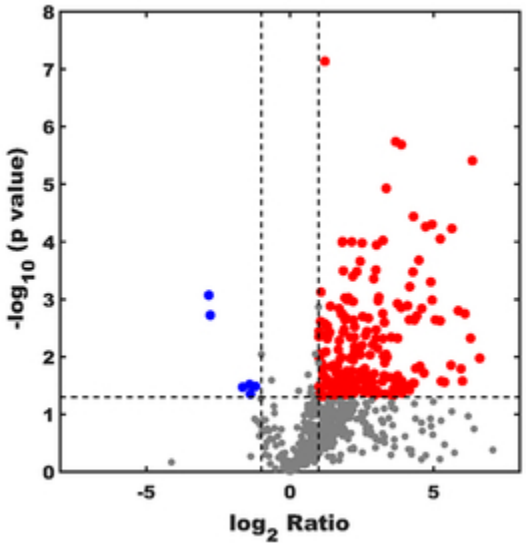

Figure 8. Volcano plot of the relative protein abundance changes between the D21+PVY and CK+PVY treatments. The red points show significantly up-regulated proteins, whereas the blue points show significantly down-regulated proteins.

34x24mm (300 x 300 DPI)

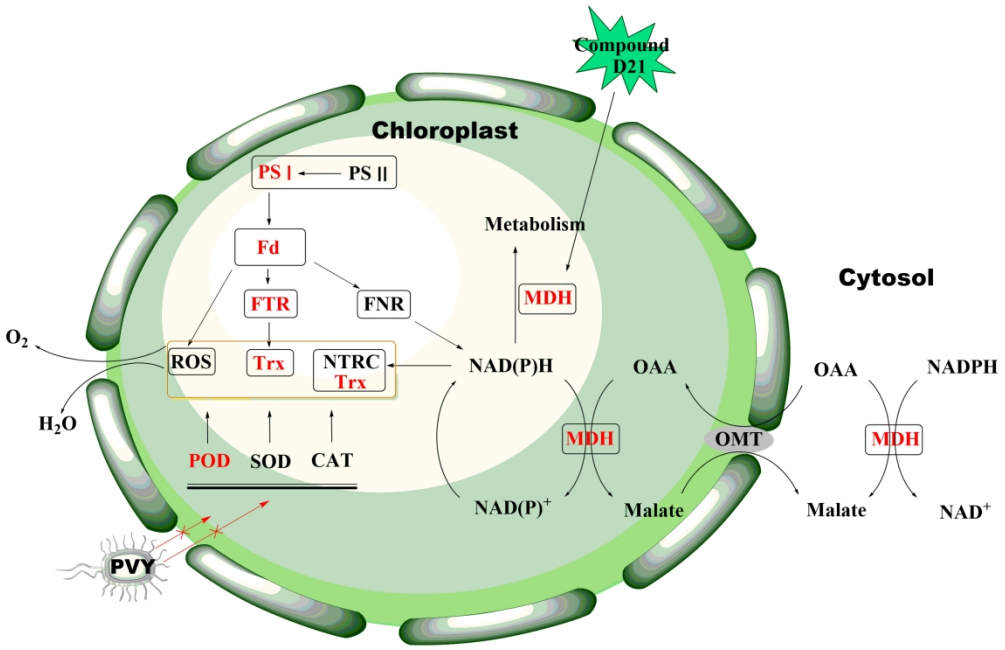

Figure 9. MDH signaling pathway in tobacco response to D21. Red color represents the up-regulated proteins in this pathway. (Fd, Ferredoxin; FNR, ferredoxin-NADP reductase; FTR, Ferredoxin-thioredoxin reductase; MDH, malate dehydrogenase; NTRC, chloroplast NADPH-thioredoxin reductase; OAA, oxaloacetate; OMT, malate/OAA translocators; PS Ⅰ, photosystem Ⅰ; PS Ⅱ, photosystem Ⅰ; ROS, reactive oxygen species; Trx, thioredoxin).

210x136mm (300 x 300 DPI)

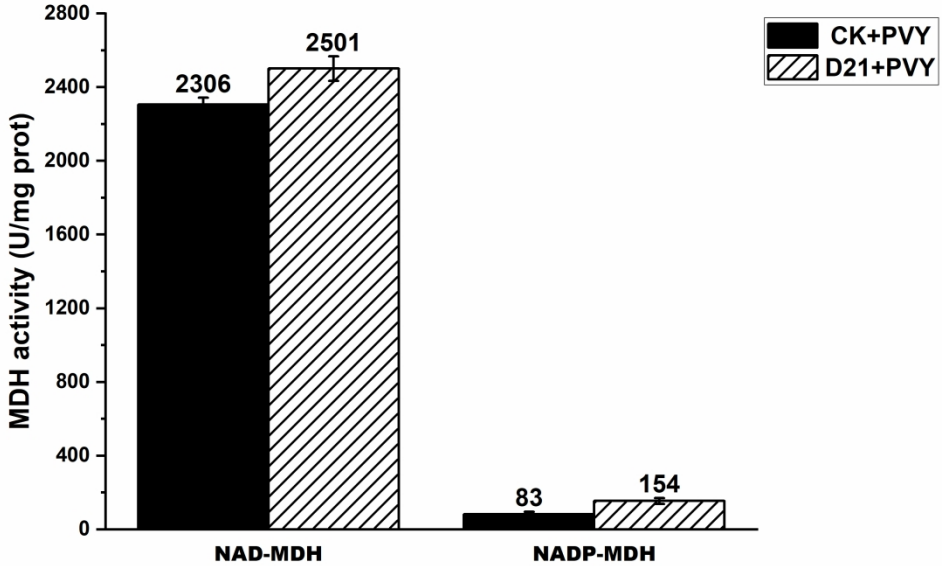

Figure 10. D21 effects on the NAD-MDH and NADP-MDH activities of tobacco leaves at day 3. Straight bars signify mean ± SD (n= 3).

272x208mm (300 x 300 DPI)

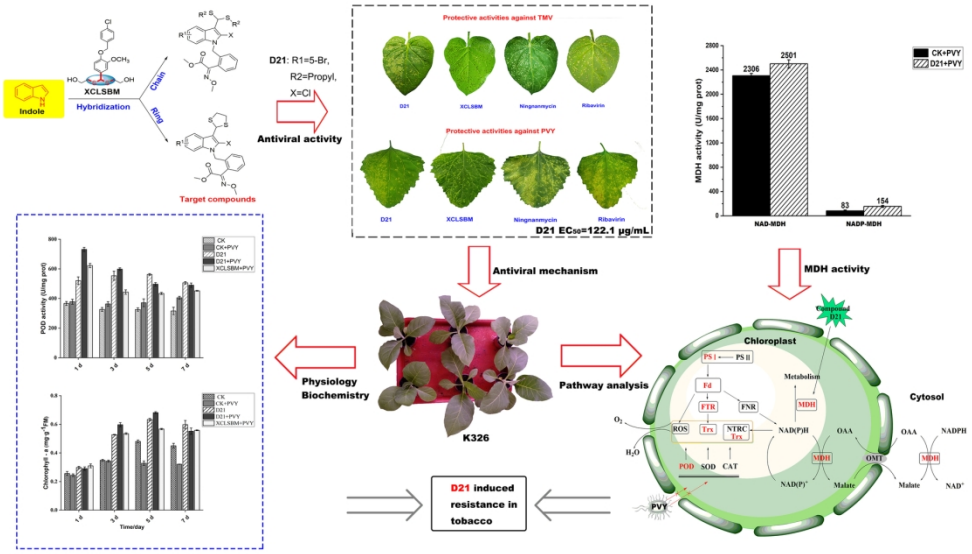

84x47mm (600 x 600 DPI)

Synthesis, Antiviral Activity and Induction of Plant Resistance of Indole Analogues Bearing Dithioacetal Moiety

Chunle Wei, Jian Zhang, Jing Shi, Xiuhai Gan, Deyu Hu,* Baoan Song *

State Key Laboratory Breeding Base of Green Pesticide and Agricultural Bioengineering, Key Laboratory of Green Pesticide and Agricultural Bioengineering, Ministry of Education, Guizhou University, Huaxi District, Guiyang 550025, China.

*Corresponding author (Tel.: 86-851-88292170; Fax: 86-851-88292170; E-mail: dyhu@gzu.edu.cn; songbaoan22@yahoo.com).

23 **ABSTRACT**: A series of compounds with potential activity to induce plant resistance
24 was synthesized from indole and thiol compounds, and methodically evaluated for
25 antiviral activity. The results indicated that some of the synthesized compounds had
26 high anti-potato virus Y (PVY), anti-cucumber mosaic virus (CMV) and anti-tobacco
27 mosaic virus (TMV) activities. Notably, compound **D21** exhibited the best activity
28 against PVY among these compounds in vivo, and the 50% effective concentrations
29 (EC_{50}) of protection activity is 122 μg/mL, which was distinctively better than the
30 corresponding values for Ribavirin (653 μg/mL), Ningnanmycin (464 μg/mL), and
31 Xiangcaoliusuobingmi (279 μg/mL). Interestingly, we found the protection activity of
32 **D21** was associated with improvement of chlorophyll content and defense-related
33 enzyme activities. Moreover, **D21** could trigger the malate dehydrogenase (MDH)
34 signaling pathway, as further confirmed by the MDH activity evaluation. Hence, **D21**
35 can protected plants against viral activity, and has potential as a novel activator for
36 plant resistance induction.

37 **KEYWORDS**: *indole, dithioacetal, antiviral activity, plant resistance induction,*
38 *malate dehydrogenase.*

39

40

41

42

43

44

45 **INTRODUCTION**

46 Plant viruses cause heavy losses throughout the history of agricultural development.
47 Potato virus Y (PVY), cucumber mosaic virus (CMV), and tobacco mosaic virus
48 (TMV) are common plant viruses that affect crop quality and yield in many areas of
49 the world[1]. Especially, PVY causes significant problems in terms of economic losses
50 in a broad range of important crops. It has a wide host range and naturally causes
51 substantial damage in tobacco, tomato, and pepper[2]. The methods used to reduce the
52 incidence of viral disease are based on chemical agents, such as Ningnanmycin and
53 Ribavirin (Figure 1), but show unsatisfactory field efficacy[3-5]. Therefore, novel,
54 highly active, and environmentally friendly antiviral agents need to be developed to
55 manage the risk of a virus epidemic.

56 **Figure 1**

57 Natural products and their derivatives have a long history as important sources of
58 and inspiration for the discovery of novel agrochemicals. The demand for new
59 nature-derived agrochemicals and environmentally friendly sources has increased
60 owing to the increasingly stringent environmental, toxicological, and regulatory
61 requirements[6-9]. Indole (Figure 1) skeleton and its derivatives occur broadly in many
62 natural products, plants, animals, and marine organisms[10]. Indole derivatives comprise
63 an important class of active compounds in heterocyclic compounds, which are
64 associated with pharmacological activities[11], such as antiviral[4, 5, 12, 13], protein kinase
65 inhibitory[14], antibacterial[15, 16], and anticancer activities[17-19]. Considering the important
66 active structures, indoles may have the most important structure category in drug

67 discovery[20-22]. Indole derivatives have a unique property that mimics the structure of
68 peptides, and it reversibly binds to enzymes[23, 24], thus, they have attracted the attention
69 of pharmacologists.

70 In our previous work, the novel dithioacetal derivative Xiangcaoliusuobingmi
71 (XCLSBM) (Figure 2) was discovered as an efficient antiviral agent[25, 26]. As an
72 extension to our research in dithioacetal and systematic study of dithioacetal
73 derivatives, a series of compounds with potential activator to induce plant resistance
74 was designed based on lead compound XCLSBM and synthesized (Figure 2) from
75 indole and 10 kinds thiol compounds. Their antiviral activities against PVY, CMV
76 and TMV and effect on defense-related enzyme activity, chlorophyll content, and
77 differentially expressed proteins (DEPs) were investigated in this study.

78 **Figure 2**

79 **MATERIALS AND METHODS**

80 **Chemicals and Instruments.** ^{1}H, and ^{13}C NMR spectra were obtained using a 500
81 or 400-MHz (100 MHz for ^{13}C) instrument (Bruker, Germany) in acetone-d_6,
82 DMSO-d_6 or $CDCl_3$ solution at room temperature. Tetramethylsilane was the internal
83 standard. HRMS was performed with Thermo Scientific Q Exactive (Thermo
84 Scientific, USA). The melting points were measured using the WRX-4 equipment
85 (Shanghai Yice Apparatus & Equipment Co., Ltd., Songjiang District, Shanghai,
86 China; uncorrected). Indolin-2-one (98% purity; CAS: 59-48-3) and other raw
87 material compounds were purchased from Aladdin Chemicals Co. (China). All
88 reagents were used without further purification and were dried before use unless

89 otherwise stated.

90 **General Procedure for Intermediates A1–A4, B, and C1–C4.** The synthetic
91 route for a novel indole series containing dithioacetal moiety is shown in Figure 3.
92 The synthesis of intermediates **A1–A4** was based on previously reported methods[27].
93 Intermediate **B** has been widely reported[28]. Intermediates **B** (5 mmol) and substituted
94 1*H*-indole-3-carbaldehyde (5 mmol) were added into acetonitrile (30 mL) with
95 potassium carbonate (6 mmol) and were heated to reflux, until the reaction was
96 completion. Then, the solvent was concentrated in vacuo, and the solids were washed
97 with water and filtered. Intermediates **C1−C4** were recrystallized from ethanol.

98 **General Synthesis Procedure for the Indole Derivatives Containing**
99 **Dithioacetal Moiety D1−D27.** Various types of thiol compounds (1.38 mmol) were
100 selectively converted to intermediates **C1−C4** (0.519 mmol) in dichloromethane (25
101 mL) in the presence of $NaHSO_4/SiO_2$ (0.01 mmol) at room temperature. Upon
102 reaction completion, silica was removed via filtration, and the filtrate was evaporated.
103 Crude products were purified by using flash chromatography with EtOAc/*n*-hexane
104 (1:3, *v*/*v*) to obtain **D1−D25** (Figure 3).

105 **Figure 3**

106 **General Synthetic Procedures for D26−D28.** 1,2-Ethanedithiol (1.38 mmol) was
107 selectively converted to intermediates **C1−C3** (0.519 mmol) in dichloromethane (25
108 mL) in the presence of $NaHSO_4/SiO_2$ (0.01 mmol) at room temperature. Upon
109 reaction completion, silica was removed by filtration, and the filtrate was evaporated.
110 The crude product was purified via flash chromatography with EtOAc/*n*-hexane (1:3,

111 *v*/*v*) to obtain the target compounds **D26−D28** (Figure 4).

112 **Figure 4**

113 **Antiviral Activity Assay.** *Extraction of PVY*[29] *and CMV*[30]. Viruses were
114 propagated in *Nicotiana. tabacum* cv. K326, ground in phosphate buffer and filtered
115 with a double-layer pledget. The extract was centrifuged for 5 min at 10000×g, and
116 the supernatant was used as the crude extract of the virus. The extraction process was
117 carried out at 4 ℃.

118 *Extraction of TMV*[31]. Viruses were propagated in *Nicotiana. tabacum* cv. K326,
119 ground in phosphate buffer and filtered with a double-layer pledget. The extract was
120 centrifuged for 5 min at 10000×g, treated twice through polyethylene glycol 6000,
121 and then centrifuged again. The extraction process was carried out at 4 ℃. The
122 absorbance values were tested using an ultraviolet spectrophotometer at 260 nm:

$$\text{Virus concentration (mg mL}^{-1}) = \frac{A_{260} \times \text{dilution ratio}}{E^{0.1\%}{}_{1\text{cm}}{}^{260\text{nm}}}$$

123

124 where E represents the extinction coefficient for TMV; $E^{0.1\%}{}_{1cm}{}^{260nm}$ is 3.1.

125 *Curative Activities of Target Compounds against PVY and CMV*[32] *in vivo.*
126 *Chenopodium amaranticolor* plants were used to evaluate the anti-PVY and
127 anti-CMV activities. The crude extracts of PVY (CMV) were dipped and inoculated
128 on the whole leaves, which were scattered with silicon carbide beforehand. The leaves
129 were washed with water after inoculation for 30 minutes and then dried. The target
130 compound solution was smeared on the right side of the leaves, and solvent was
131 smeared on the left side, which served as the control. All the plants were cultivated in
132 an incubator under an illumination of 10 000 lx at 28±2 ℃. The number of local

133 lesions appearing 5 to 6 days after inoculation was counted. Measurements were
134 performed in triplicate.

135 *Protective Activities of Target Compounds against PVY and CMV in vivo.* The
136 target compound solution was smeared on the right side of the leaves, and solvent was
137 smeared on the left side, which served as the control. *Chenopodium amaranticolor*
138 plants were inoculated with PVY (CMV) after 24 hours. The leaves were washed with
139 water after inoculation for 30 minutes. All the plants were cultivated in an incubator
140 under an illumination of 10 000 lx at 28±2 ℃. The number of local lesions appearing
141 5 to 6 days after inoculation was counted. Measurements were performed in triplicate.
142 Measurements were performed in triplicate.

143 *Curative Activities of Target Compounds against TMV in vivo. Nicotiana. tabacum*
144 L. plants were used to evaluate the anti-TMV activities. TMV at a concentration of
145 6×10^{-3} mg mL^{-1} was dipped and inoculated on the whole leaves, which were
146 scattered with silicon carbide beforehand. The leaves were washed with water after
147 inoculation for 30 minutes and then dried. The target compound solution was smeared
148 on the right side of the leaves, and solvent was smeared on the left side, which served
149 as the control. All the plants were cultivated in an incubator under an illumination of
150 10 000 lx at 28±2 ℃. The number of local lesions appearing 3 to 4 days after
151 inoculation was counted. Measurements were performed in triplicate.

152 *Protective Activities of Target Compounds against TMV in vivo.* The target
153 compound solution was smeared on the right side of the leaves, and solvent was
154 smeared on the left side, which served as the control. *Nicotiana. tabacum* L. plants

155 were inoculated with TMV after 24 hours. The leaves were washed with water after
156 inoculation for 30 minutes. All the plants were cultivated in an incubator under an
157 illumination of 10 000 lx at 28±2 ℃. The number of local lesions appearing 3 to 4
158 days after inoculation was counted. Measurements were performed in triplicate.
159 Measurements were performed in triplicate.

160 The inhibitory rate of each compound was calculated as follows ('av' means
161 average):

$$\text{Inhibition rate } (\%) = \frac{\text{av no.of local lesions of control (not treated with compound)} - \text{av no.of lesions smeared with compound}}{\text{av no.of local lesions of control (not treated with compound)}} \times 100\%$$

162

163 **Physiological and Biochemical Analysis.** *Compound Treatments and Sampling.*
164 *Nicotiana. tabacum* cv. K326 plants were selected until the four- to six-leaf stage.
165 Exactly 500 μg/mL of **D21** solution was sprayed on the plants, comprising the
166 treatment group, whereas XCLSBM and water belonged to the positive and negative
167 (CK) controls, respectively. The five treatments were **CK**, **D21**, **CK+PVY**,
168 **XCLSBM+PVY**, and **D21+PVY**. Plant leaves were collected at 1, 3, 5, and 7 days
169 after infection with PVY for the defensive enzyme activity assay, and to determine the
170 chlorophyll content and DEPs. All the test plants were cultivated in an incubator
171 under an illumination of 10 000 lx at 28±2 ℃. Measurements were repeated in
172 triplicate.

173 *Determination of Enzyme Activities.* The activities of catalase (CAT), phenylalanine
174 ammonia lyase (PAL), peroxidase (POD), and superoxide dismutase (SOD) were
175 tested using enzyme assay reagent kits (Suzhou Comin Bioengineering Institute,

176 Jiangsu, China). MDH activity assay was performed based on the reagent kits from
177 Beijing Solarbio Science & Technology Co., Ltd.

178 *Chlorophyll Content Test.* Chlorophyll content assay was conducted as previously
179 described[33]. The absorption spectra of chlorophyll a (C_a) and b (C_b) were detected at
180 663 and 645 nm, respectively, and chlorophyll total (C_t) were calculated as: $C_t = C_a + C_b$.
181 Measurements were performed in triplicate.

182 **DEPs Analysis.** *Extraction of Total Tobacco Protein.* Total tobacco proteins were
183 extracted as previously described with slight modification[31, 32]. Approximately 1.5 g
184 of leaf sample was ground in liquid nitrogen to power, and homogenized in 5 mL
185 sucrose lysis buffer (0.04 M dithiothreitol, 0.05 M EDTA, 100 mM KCl, 500 mM
186 Tris-HCl, 700 mM sucrose, pH 7.5) at 25 ℃ for 30 minutes. 5 mL of Tris–phenol was
187 added, and then shaken for 30 minutes at 4 ℃. Centrifugation for 8 minutes at 6000
188 rpm, the upper phenol layer was collected. Five volumes of 100 mM ice-cold
189 ammonium acetate in methanol was added, and the sample was stored for 12 hours at
190 -20 ℃. Then the sample was centrifuged at 4 ℃ and 6000 rpm for 15 minutes. The
191 precipitate was collected and washed thrice with cold acetone. The precipitate was
192 dried in Speed Vac (SIM International Group Co., Ltd., NJ, USA) for 5 hours and
193 solubilized in 1 mL of rehydration solution (PH 8.5, 0.04 M DTT, 0.1 M Tris, 8 M
194 urea) for 50 minutes at 37 °C. Protein concentration was measured by the Bradford
195 method. Afterward, solutions containing 100 μg proteins were collected and alkylated
196 with equal volume of 55 mM iodoacetamide. The mixture was incubated at 25 ℃ for
197 40 minutes in the dark, and then centrifuged with 3 kDa Millipore for 20 minutes at

198 12000 rpm and 4 °C. Next, the protein was digested in 40 μL of 25 mM NH_4HCO_3
199 with 5 μg of trypsin (Promega, Madison, USA) at 37 °C and 800 rpm for 8 hours. The
200 suspension was centrifuged for 40 minutes at 12000 rpm and 4 ℃. Finally, peptide
201 solution was collected, dried, and solubilized in 45 μL of H_2O (LC/MS grade)
202 containing 0.1 % formic acid (FA) for liquid chromatography-tandem MS
203 (LC-MS/MS) analysis.

204 *Protein Identification.* Every peptide sample was resolved using a Nano
205 LC-1DTM plus system with triple-of-flight 5600 mass spectrometer (AB Sciex,
206 Foster City, CA, USA). Then, peptide (8 μL) was obtained via a full-loop injection
207 and then desalted on a ChromXP Trap column (Nano LC TRAP Column, 0.5
208 mm×350 μm, 3 μm C18-CL, 120 Å, AB Sciex, Foster City, CA, USA). The sample
209 was washed into a second analytical column (3C18-CL column, 15 cm ×75 μm, AB
210 Sciex, Foster City, CA, USA) by using a linear gradient composed of mobile phase
211 A (0.1 % FA, 95% ACN) and B (0.1 % FA, 5 % ACN) for 1.5 h at a flow rate of 5
212 nL/s. Three times TOF 5,600 MS was ran in data-dependent mode to conversion
213 between product ion acquisition and TOF-MS by using the Analyst (R) software
214 (TF1.6) (AB SCIEX, Foster City, CA, USA). Beta-galactosidase digestion was used
215 to calibrate each pair of samples by elution for 10 min and identification for 30
216 minutes.

217 *Proteomics Data Analysis.* The MaxQuant[34] version 1.5.2.8 of the Andromeda
218 search engine was used, and the LC-MS/MS data was analyzed and quantified based
219 on the PVY proteome downloaded from UniProt (http://www.uniprot.org/). In

220 Andromeda's main research, the original mass tolerances for the debris and mass of
221 precursors are 20 and 6 ppm, respectively. The global false discovery rate (FDR)
222 cut-off was set to 0.01 in protein and peptide identification. Normalized protein
223 intensity was decided via label-free quantification[35]. The algorithm of the
224 intensity-based absolute quantification (iBAQ) was sorted with the absolute
225 abundance of DEPs[36]. Protein tables were filtered by eliminating identifications of
226 common contaminants and reverse database. Differentially accumulated proteins
227 were identified by Unpaired two-samples t-test of iBAQ data between control and
228 treatment groups.

229 *Bioinformatics Analysis.* For functional analyses, we used cluster samples to test
230 the increase/decrease in DEPs common for all three replicates. The Kyoto
231 Encyclopedia of Genes and Genomes (KEGG) annotation was retrieved from the
232 KEGG Pathway database (http://www.genome.jp/Pathway). The databases were
233 searched using the Uniprot software.

234 **RESULTS AND DISCUSSION**

235 **Chemistry.** Figure 3 shows the synthetic routes of indole derivatives containing a
236 dithioacetal group. 2-Chloro, 2-bromo, 5-bromo-2-chloro, and 2-methyl-1H-indole-3-
237 carbaldehyde **A1–A4** were synthesized via Vilsmeier–Haack reaction to determine the
238 effects of electron-donating and electron-withdrawing groups on the antiviral activity.
239 **C1–C4** were obtained by stirring and refluxing the corresponding **A1–A4**, **B**, and
240 potassium carbonate in acetonitrile for about 3 hours to obtain a yield of 87 % to 93 %.
241 To systematically study the effect of dithioacetal structure on the virus, we

242 synthesized the target compounds **D1–D25** via **C1–C4** and nine different thiols
243 (mercaptoethanol, ethyl mercaptan, propanethiol, isopropyl mercaptan,
244 1,2-ethanedithiol, 4-chlorothiophenol, 2,4-dichlorothiophenol, butyl mercaptan,
245 *n*-butyl mercaptan, and dodecyl mercaptan) via Michael addition and achieved a yield
246 of 70 %–95 %. The dithioacetal moiety was further synthesized into a closed loop
247 (Figure 4). The chemical structures of key intermediates **C1–C4** and target
248 compounds **D1–D28** were identified by NMR and HRMS (Supporting Information
249 Ⅰ).

250 **Antiviral Activity.** *Anti-PVY Activity in Vivo*. The anti-PVY activities of **D1–D28**
251 are summarized in Table 1. **D21** displayed higher antiviral curative activities against
252 PVY with values of 61.6 %, than that of Ningnanmycin (50.1 %), Ribavirin (40.2 %),
253 and lead compound XCLSBM (55.2 %). **D21** exhibited excellent protective activities
254 on PVY with values of 70.1 %, superior to Ningnanmycin (50.8 %), Ribavirin (41.2
255 %), and lead compound XCLSBM (57.7 %).

256 **Table 1**

257 To further confirm the anti-PVY activity of the target compounds, the EC_{50} of the
258 target compounds anti-PVY were tested and the results were listed in Table 2.
259 Evidently, **D5**, **D21**, and **D24** exhibited good curative activity anti-PVY with EC_{50}
260 values of 272, 217, and 288 μg/mL, respectively, which higher than that of Ribavirin
261 (686 μg/mL), Ningnanmycin (468 μg/mL), and lead compound XCLSBM (292
262 μg/mL). **D2**, **D21**, **D23**, and **D24** exhibited higher protective activity anti-PVY with
263 EC_{50} of 212, 122, 268, and 244 μg/mL, respectively, than that of Ribavirin (653

264 μg/mL), Ningnanmycin (464 μg/mL), and lead compound XCLSBM (279 μg/mL).

265 *Anti-CMV Activity in Vivo.* The anti-CMV activities of **D1–D28** are displayed in
266 Tables 1 and 2. The protective activities of **D2**, **D11**, and **D21** with EC_{50} of 187, 200,
267 and 156 μg/mL, respectively, which were higher than that of Ribavirin (690 μg/mL),
268 Ningnanmycin (439 μg/mL), and lead compound XCLSBM (240 μg/mL). The
269 curative effects of **D2**, **D3**, **D5**, **D9**, **D11**, **D12**, **D19**, **D20**, and **D21** with EC_{50} levels of
270 199, 220, 202, 194, 225, 224, 217, 202, and 179 μg/mL, respectively, also surpassed
271 that of Ribavirin (704 μg/mL), Ningnanmycin (498 μg/mL), and lead compound
272 XCLSBM (275 μg/mL).

273 *Anti-TMV Activity in Vivo.* The anti-TMV activities of **D1–D28** were measured
274 and shown in Tables 1 and 2. The protective activities anti-TMV EC_{50} values of **D10**,
275 **D19**, and **D21** is 207, 212, and 200 μg/mL, respectively, which similar to
276 Ningnanmycin (198 μg/mL), but higher than that of Ribavirin (568 μg/mL) and lead
277 compound XCLSBM (497 μg/mL). **D1-D3**, **D5**, **D10**, **D12**, **D14**, **D19–D23**, and **D25**
278 had curative activities with EC_{50} levels of 225, 255, 209, 215, 322, 220, 364, 342, 212,
279 209, 293, 293, and 241 μg/mL, respectively, which were higher than that of Ribavirin
280 (668 μg/mL), Ningnanmycin 382 μg/mL), and lead compound XCLSBM (517
281 μg/mL).

282 **Table 2**

283 *Structure−Activity Relationships (SARs)*. Results of preliminary SARs illustrated
284 that the presence of different thiol compounds influenced the anti-PVY activity of
285 indole derivatives containing dithioacetal moiety. This notion was proven by the

286 following data, **D21** (R^2 = Propyl) > **D17** (R^2 = Tert-butyl), **D24** (R^2 = Propyl) > **D8**
287 (R^2 = Tert-butyl). Thiol compounds in a linear chain had higher antiviral activity than
288 non-directly linked thiol compounds in which **D3** (R^2 = Propyl) > **D4** (R^2 = Isopropyl),
289 **D12** (R^2 = Propyl) > **D13** (R^2 = Isopropyl), **D16** (R^2 = Butyl) > **D17** (R^2 = Tert-butyl).
290 No change was observed in terms of the activity when electron-withdrawing (halogen)
291 or donating (methyl group) groups were introduced at the 2 position of the indole.
292 This phenomenon was verified by the following data, **D10** (X = Br) ≈ **D22** (X = CH_3),
293 **D2** (X = Cl) ≈ **D23** (X = CH_3), and **D5** (X = Cl) ≈ **D25** (X = CH_3). The closed-loop
294 structure of dithioacetals were not contribute to antiviral activity (**D26**, **D27**, and **D28**
295 have weak antiviral activity). Hence, the dithioacetal structures are essential for
296 inducing plant resistance, and when R^1 = Br, R^2 = Propyl, and X = Cl, the target
297 compound was the best activator for plant resistance induction.

298 **Physiological and Biochemical Analysis.** Plants' immune system is activated
299 when infected with various aggressive pathogens. A range of defense responses can
300 cause strong physiological and biochemical changes in green plants, which can
301 significantly increase chlorophyll content and defense enzyme activity[39,40].

302 *Effect on Chlorophyll Contents.* Chlorophyll content is closely related to
303 photosynthesis and plays a major role in the growth process of plants. C_a, C_b, and C_t
304 content (Figure 5) decreased after PVY infected the *Nicotiana tabacum* cv. K326
305 plants in our study. In the **D21** and **D21+PVY** groups, chlorophyll content gradually
306 increased from day 1 to day 5, and the maximum content was observed on day 5
307 (Figure 5A-C). So, **D21** can increase chlorophyll content and promote photosynthesis,

308 thereby enhancing defense responses and promoting plant host disease resistance.

309 **Figure 5**

310 *Influences of Defense Enzyme Activity.* Induced resistance is associated to enhance
311 activities of defensive enzymes, such as SOD, POD, PAL, and CAT. SOD is a
312 superoxide anion scavenging enzyme. POD can eliminate the toxicity of hydrogen
313 peroxide, phenols and amines to plants. PAL plays an important role in the normal
314 growth and development of plants and resists bacterial infection. And CAT can
315 scavenge reactive oxygen species. The antioxidant defense mechanisms of these
316 enzymes protect plants from oxidative stress induced by reactive oxygen species
317 (ROS)[41]. Hence, we systematically analyzed the defense enzyme activity of *Nicotiana*
318 *tabacum* cv. K326 after **D21** treatment. After being infected by PVY, the SOD
319 activity of tobacco increased slightly on the first day and then decreased. After **D21**
320 treatment, the SOD activity of **D21** group was remarkably higher than that of the
321 **CK+PVY** group, which reached the maximum on the 3rd day and increased by 46.6%
322 compared with **CK** group (Figure 6A). The POD activities of the **CK+PVY**,
323 **D21+PVY**, and **XCLSBM+PVY** groups notably increased after infecting the tobacco
324 plant with PVY. Simultaneously, the **D21+PVY** and **XCLSBM+PVY** groups reached
325 the maximum (731 and 622 U/mg prot) on the first day. The POD activity of the **D21**
326 and **D21+PVY** groups were higher than that of the **CK** and **CK+PVY** groups,
327 respectively, during the first to the 7th day (Figure 6B). The PAL activities of the **D21**,
328 **D21+PVY** and **XCLSBM+PVY** groups were higher than those of the **CK** group. The
329 **D21+PVY** group had the highest activity. The **D21+PVY** group reached maximum

330 on the third day, which was 95.3% higher than the **CK+PVY** group (Figure 6C).
331 After PVY infection, the CAT activities of the **D21** and **D21+PVY** groups increased
332 than those of the other treatment groups during the monitoring period. The CAT
333 activity of D21, D21+PVY and XCLSBM+PVY treatments first increased and then
334 decreased during the monitoring period, and reached the maximum on the third day
335 (Figure 6D). The results of defense enzyme activity evaluation indicated that **D21** can
336 increase the activities of some defensive enzymes (SOD, POD, PAL, and CAT),
337 thereby enhancing defense responses and improving plant resistance.

338 **Figure 6**

339 **Proteomics Analysis.** In the determination of physiological and biochemical
340 properties, the most remarkable change in tobacco after **D21** treatment was observed
341 on the third day. Therefore, the total proteins of the **CK+PVY** and **D21+PVY** groups
342 on the third day were analyzed through label-free LC-MS/MS. The results displayed
343 that 844 proteins were identified (Supporting Information Ⅱ, Table 2). A total of 785
344 and 733 proteins were identified in the **D21+PVY** and **CK+PVY** groups, respectively
345 (Figure 7). In total, 111 (13.2 %) and 59 (7 %) proteins were discovered in the
346 **CK+TMV** and **D21+TMV** groups, respectively.

347 **Figure 7**

348 Figure 8 shows that the down-regulated (blue dots) and up-regulated (red dots) ($p <$
349 0.05, fold changes > 2.0) in the different treatment groups were 6 and 201 in the
350 **CK+PVY** and **D21+PVY** groups, respectively. To determine the expression levels of
351 these DEPs, a volcanic map was employed.

352 **Figure 8**

353 **Functional Classification by KEGG.** The possible biological pathway of DEPs
354 between the **D21+PVY** and **CK+PVY** groups were identified via KEGG analysis.
355 The mode of action triggered by **D21** was determined. The KEGG database categories
356 mapped DEPs at a level of $P < 0.05$. As shown in Table 3 and Figure 10, five MDHs
357 (EC 1.1.1.37), Malic enzyme, four Thioredoxin (Trxs), calvin cycle protein CP12-3,
358 Ferredoxin (Fd), two Ferredoxin-thioredoxin reductases (FTRs), four NADH
359 dehydrogenases, Peroxidase (EC 1.11.1.7) (POD), five Peroxiredoxins (EC 1.11.1.15)
360 (Prxs), and photosystem Ⅰ reaction center subunit IV B (PS Ⅰ) were upregulated.
361 These specific proteins played an important role in the MDH signaling pathway
362 (Figure 9). They can catalyze the reversible conversion between oxaloacetate (OAA)
363 and malate, which are involved in photosynthesis, C4 cycle, TCA cycle, and other
364 metabolic pathways[43, 44]. The electron transfer components from photosystem I to the
365 target enzyme are ferredoxin, FTRs and thioredoxin[45]. Calvin cycle protein CP12-3
366 acts as a linker and is essential in the assembly of a core complex of PRK/GAPDH.
367 The reversible inactivation of chloroplast enzymes GAPDH and PRK is coordinated
368 during darkness in photosynthetic tissues[46]. Trxs are widely present in plant
369 chloroplasts, and photosynthetic enzymes are photoregulated by FTRs. Trxs are
370 critical for the redox regulation of protein function and signaling through thiol redox
371 regulation[47]. NADH dehydrogenases are involved in the electron transport from
372 light-produced NADPH and Fd to the intersystem plastoquinone pool[48]. The
373 H_2O_2-decomposing antioxidant enzyme group consisted of Prxs. Prx proteins

374 disintegrate peroxynitrites and alkyl hydroperoxides and lead to reduction in H_2O_2[49].
375 PODs increase the plant defense against pathogens by reducing some aromatic
376 compounds (electron donors) and the toxicity of peroxides, and catalyzing the ability
377 of H_2O_2-dependent redox reduction[50]. In this study, **D21** increased the protein to
378 regulate the expression level of the MDH and photoreaction system in the chloroplast.
379 Moreover, **D21** increased the defense enzyme activity, thereby increasing plant
380 disease resistance.

381 **Table 3**

382 **Figure 9**

383 **MDH Activity.** To verify the effect of **D21** on the MDH signaling pathway, we
384 tested the NADP-MDH and NAD-MDH activities. Results (Figure 10) showed that
385 the NAD-MDH and NADP-MDH activities of the **D21+PVY** group increased by
386 8.4% and 85.5%, respectively, compared with the **CK+PVY** group on the third day
387 after PVY infection. **D21** increased the MDH activity and acted on the MDH
388 signaling pathway.

389 **Figure 10**

390 In summary, Twenty-eight novel indole derivatives containing dithioacetal moiety
391 were designed, synthesized, and their activities against plant viruses were evaluated
392 methodically. Bioassay results indicated that **D21** exhibited higher antiviral protective
393 activity than others target compounds, and superior to the commercial Ribavirin,
394 Ningnanmycin, and lead compound XCLSBM. The excellent antiviral protective
395 activity of **D21** was attributed to potential activator for plant resistance induction,

396 which was associated with improvement of chlorophyll content and defense enzyme
397 activities in tobacco treated with **D21**. KEGG analysis indicated that **D21+PVY**
398 versus **CK+PVY** group regulated the stress response and related proteins of the MDH
399 signaling pathway, as confirmed by the MDH activity evaluation. Therefore, **D21** has
400 potential as a novel type of antiviral agent for plants.

401 **CONTENT ASSOCIATED**

402 **Supporting Information**

403 ^{1}H NMR and ^{13}C NMR spectrum of intermediate **C1-C4** and target compound
404 **D1−D28** are shown in Supplementary Information I. All identified proteins are shown
405 in Support Information II.

406 **AUTHOR INFORMATION**

407 **Corresponding Authors**

408 *E-mail for Baoan Song: songbaoan22@yahoo.com. *Phone: 86-851-88292170. Fax:
409 86-851-83622211.
410 *E-mail for Deyu Hu: dyhu@gzu.edu.cn. *Phone: 86-851-8829-2170. Fax:
411 86-851-88292170.

412 **ORCID**

413 Baoan Song: 0000-0002-4237-6167
414 Deyu Hu: 0000-0001-7843-371X

415 **ACKNOWLEDGMENT**

416 This study was supported by the National Natural Science Foundation of China (No.
417 21867002).

418 **Notes**

419 The authors declare no competing financial interest.

420 **ABRREVIATIONS**

421 PVY, potato virus Y; CMV, Cucumber mosaic virus; TMV, tobacco mosaic virus;
422 EC_{50}, effective concentrations; XCLSBM, Xiangcaoliusuobingmi; SOD, superoxide
423 dismutase; POD, peroxidase; PAL, phenylalanine ammonia lyase; CAT, catalase; C_a,
424 chlorophyll a; C_b, hlorophyll b; Ct, chlorophyll total; DEPs, differentially expressed
425 proteins; FDR, false discovery rate; iBAQ, intensity-based absolute quantification;
426 KEGG, Kyoto Encyclopedia of Genes and Genomes; SARs, Structure−activity
427 Relationships; Fd, Ferredoxin; FNR, ferredoxin-NADP reductase; FTR,
428 Ferredoxin-thioredoxin reductase; MDH, malate dehydrogenase; NTRC, chloroplast
429 NADPH-thioredoxin reductase; OAA, oxaloacetate; OMT, malate/OAA translocators;
430 PS Ⅰ, photosystem Ⅰ; PS Ⅱ, photosystem Ⅰ; ROS, reactive oxygen species; Trx,
431 thioredoxin; TCA, tricarboxylic acid cycle; GAPDH, glyceraldehyde-3-phosphate
432 dehydrogenase; PRK, phosphoribulokinase.

434 **REFERENCES**

435 (1) Gray, S.; Boer, S. D.; Lorenzen, J.; Karasev, A.; Whitworth, J.; Nolte, P.; Singh,
436 R.; Boucher, A.; Xu, H. M. Potato virus Y: an evolving concern for potato crops
437 in the United States and Canada. *Plant Dis*. **2010**, 94, 1384-1397.

438 (2) Scholthof, K. B. G.; Adkins, S.; Czosnek, H.; Palukaitis, P.; Jacquot, E.; Hohn, T.;
439 Hohn, B.; Saunders, K.; Candresse, T.; Ahlquist, P.; Hemenway, C.; Foster, G. D.
440 Top 10 plant viruses in molecular plant pathology. *Mol. Plant Pathol.* **2011**, 12,
441 938-954.

442 (3) Wu, Z. X.; Zhang, J.; Chen, J.; Pan, J. K.; Zhao, L.; Liu, D. Y.; Zhang, A. W.;
443 Chen, J. X.; Hu, D. Y.; Song, B. A. Design, synthesis, antiviral bioactivity and
444 three-dimensional quantitative structure-activity relationship study of novel ferulic
445 acid ester derivatives containing quinazoline moiety. *Pest Manage. Sci.* **2017**, 73,
446 2079-2089.

447 (4) Liu, B.; Li, R.; Li, Y. N.; Li, S. Y.; Yu, J.; Zhao, B. F.; Liao, A. C.; Wang, Y.;
448 Wang, Z. W.; Lu, A. D.; Liu, Y. X.; Wang, Q. M. Discovery of Pimprinine
449 Alkaloids as Novel Agents against a Plant Virus. *J. Agric. Food Chem.* **2019**, 67,
450 1795-1806.

451 (5) Lu, A. D.; Wang, T. N.; Hui, H.; Wei, X. Y.; Cui, W. H.; Zhou, C. L.; Li, H. Y.;
452 Wang, Z. W.; Guo, J. C.; Ma, D. J.; Wang, Q. M. Natural Products for Drug
453 Discovery: Discovery of Gramines as Novel Agents against a Plant Virus. *J. Agric.*
454 *Food Chem.* **2019**, 67, 2148-2156.

455 (6) Gerwick, B. C.; Sparks, T. C. Natural products for pest control: an analysis of
456 their role, value and future. *Pest Manage. Sci.* **2014**, 70, 1169-1185.

457 (7) Sparks, T. C.; Hahn, D. R.; Garizi, N. V. Natural products, their derivatives,
458 mimics and synthetic equivalents: role in agrochemical discovery. *Pest Manage.*
459 *Sci.* **2016**, 73, 700-715.
460 (8) Qian, X. H.; Lee, P. W.; Cao, S. China: Forward to the Green Pesticides via a
461 Basic Research Program. *J. Agric. Food Chem.* **2010**, 58, 2613-2623.
462 (9) Oliveira, J. L.; Ramos Campos, E. V.; Fraceto, L. F. Recent Developments and
463 Challenges for Nanoscale Formulation of Botanical Pesticides for Use in
464 Sustainable Agriculture. *J. Agric. Food Chem.* **2018**, 66, 8898-8913.
465 (10) Zhang, M. Z.; Chen, Q.; Yang, G. F. A review on recent developments of
466 indole-containing antiviral agents. *Eur. J. Med. Chem.* **2015**, 89, 421-441.
467 (11) Samala, S.; Arigela, R. K.; Kant, R.; Kundu, B. Diversity-oriented synthesis of
468 ketoindoloquinoxalines and indolotriazoloquinoxalines from
469 1-(2-nitroaryl)-2-alkynylindoles. *J. Org. Chem.* **2014**, 79, 2491-2500.
470 (12) Ji, X. F.; Guo, J. C.; Liu, Y. X.; Lu, A. D.; Wang, Z. W.; Li, Y. Q.; Yang, S. X.;
471 Wang, Q. M. Marine-Natural-Product Development: First Discovery of
472 Nortopsentin Alkaloids as Novel Antiviral, Anti-phytopathogenic-Fungus, and
473 Insecticidal Agents. *J. Agric. Food Chem.* **2018**, 66, 4062-4072.
474 (13) Chen, L. W.; Xie, J. L.; Song, H. J.; Liu, Y. X.; Gu, Y. C.; Wang, L. Z.; Wang, Q.
475 M. Design, Synthesis, and Biological Activities of Spirooxindoles Containing
476 Acylhydrazone Fragment Derivatives Based on the Biosynthesis of Alkaloids
477 Derived from Tryptophan. *J. Agric. Food Chem.* **2016**, 64, 6508-6516.

478 (14) Rao, V. K.; Chhikara, B. S.; Shirazi, A. N.; Tiwari, R.; Parang, K.; Kumar, A.
479 3-substitued indoles: one-pot synthesis and evaluation of anticancer and Src kinase
480 inhibitory activities. *Bioorg. Med. Chem. Lett.* **2011**, 21, 3511-3514.
481 (15) Ishikura, M.; Yamada, K.; Abe, T. Simple indole alkaloids and those with a
482 nonrearranged monoterpenoid unit. *Nat. Prod. Rep.* **2010**, 27, 1630-1680.
483 (16) Rao, V. K.; Rao, M. S.; Jain, N.; Panwar, J.; Kumar, A. Silver triflate catalyzed
484 synthesis of 3-aminoalkylated indoles and evaluation of their antibacterial activities.
485 *Org. Med. Chem. Lett.* **2011**, 1, 1-7.
486 (17) Robinson, M. W.; Overmeyer, J. H.; Young, A. M.; Erhardt, P. W.; Maltese, W.
487 A. Synthesis and evaluation of indole-based chalcones as inducers of methuosis, a
488 novel type of nonapoptotic cell death. *J. Med. Chem.* **2012**, 55, 1940-1956.
489 (18) Granchi, C.; Roy, S.; De Simone, A.; Salvetti, I.; Tuccinardi, T.; Martinelli, A.;
490 Macchia, M.; Lanza, M.; Betti, L.; Giannaccini, G.; Lucacchini, A.; Giovannetti, E.;
491 Sciarrillo, R.; Peters, G. J.; Minutolo, F. N-Hydroxyindole-based inhibitors of
492 lactate dehydrogenase against cancer cell proliferation. *Eur. J. Med. Chem.* **2011**,
493 46, 5398-5407.
494 (19) Ke, S.; Shi, L.; Cao, X.; Yang, Q.; Liang, Y.; Yang, Z. Heterocycle-functional
495 gramine analogues: solvent- and catalyst-free synthesis and their inhibition
496 activities against cell proliferation. *Eur. J. Med. Chem.* **2012**, 54, 248-254.
497 (20) Horton, D. A.; Bourne, G. T.; Smythe, M. L. The combinatorial synthesis of
498 bicyclic privileged structures or privileged substructures. *Chem. Rev.* **2003**, 103,
499 893-930.

500 (21) Fernando, R. S. A.; Eliezer, J. B.; Carlos, A. M. F. From Nature to Drug
501 Discovery: The Indole Scaffold as a 'Privileged Structure'. *Mini-Rev. Med. Chem.*
502 **2009**, 9, 782-793.
503 (22) Welsch, M. E.; Snyder, S. A.; Stockwell, B. R. Privileged scaffolds for library
504 design and drug discovery. *Curr. Opin. Chem. Biol.* **2010**, 14, 347-361.
505 (23) Kaushik, N. K.; Kaushik, N.; Attri, P.; Kumar, N.; Kim, C. H.; Verma, A. K.;
506 Choi, E. H. Biomedical importance of indoles. *Molecules* **2013**, 18, 6620-6662.
507 (24) Dolle, R. E. Comprehensive Survey of Combinatorial Library Synthesis. *J. Comb.*
508 *Chem*. **2001**, 3, 477-517.
509 (25) Zhang, J.; Zhao, L.; Zhu, C.; Wu, Z. X.; Zhang, G. P.; Gan, X. H.; Liu, D. Y.;
510 Pan, J. K.; Hu, D. Y.; Song, B. A. Facile Synthesis of Novel Vanillin Derivatives
511 Incorporating a Bis (2-hydroxyethyl) dithhioacetal Moiety as Antiviral Agents. *J.*
512 *Agric. Food Chem.* **2017**, 65, 4582-4588.
513 (26) Chen, J.; Shi, J.; Yu, L.; Liu, D. Y.; Gan, X. H.; Song, B. A.; Hu, D. Y. Design,
514 Synthesis, Antiviral Bioactivity, and Defense Mechanisms of Novel Dithioacetal
515 Derivatives Bearing a Strobilurin Moiety. *J. Agric. Food Chem.* **2018**, 66,
516 5335-5345.
517 (27) Tu, H.; Wu, S. Q.; Li, X. Q.; Wan, Z. C.; Wan, J. L.; Tian, K.; Ouyang, G. P.
518 Synthesis and Antibacterial Activity of Novel 1*H*-indol-2-ol Derivatives. *J.*
519 *Heterocyclic Chem.* **2017**, 55, 269-275.

520 (28) Lu, G. H.; Chu, H. B.; Chen, M.; Yang, C. L. Synthesis and bioactivity of novel
521 strobilurin derivatives containing the pyrrolidine-2,4-dione moiety. *Chin. Chem.*
522 *Lett.* **2014**, 25, 61-64.
523 (29) Iannelli, D.; Apice, L. D.; Cottone, C.; Viscardi, M.; Scala, F.; Zoina, A.; Sorbo,
524 G. D.; P. Spigno, P.; Capparelli, R. Simultaneous detection of cucumber mosaic
525 virus, tomato mosaic virus and potato virus Y by flow cytometry. *J. Virol. Methods*
526 **1997**, 69, 137–145.
527 (30) Scott, H. Purification of Cucumber Mosaic Virus. *Virol.* **1963**, 20, 103-106.
528 (31) Gooding, G. V.; Jr.; Hebert, T. T. A simple technique for purification of tobacco
529 mosaic virus in large quantities. *Phytopathology* **1967**, 57, 1285−1287.
530 (32) Zhang, H. P.; Wang, H.; Yang, S.; Jin, L. H.; Hu, D. Y.; Pang, L. L.; Xue, W.;
531 Song, B. A. Synthesis and antiviral activity of novel chiral cyanoacrylate
532 derivatives. *J. Agric. Food Chem.* **2005**, 53, 7886−7891.
533 (33) Zhao, J.; Zhou, J. J.; Wang, Y. Y.; Gu, J. W.; Xie, X. Z. Positive regulation of
534 phytochrome B on chlorophyll biosynthesis and chloroplast development in rice.
535 *Rice Sci.* **2013**, 20, 243−248.
536 (34) Cox, J.; Neuhauser, N.; Michalski, A.; Scheltema, R. A.; Olsen, J. V.; Mann, M.
537 Andromeda: a peptide search engine integrated into the MaxQuant environment. *J.*
538 *Proteome Res.* **2011**, 10, 1794−1805.
539 (35) Cox, J.; Michalski, A.; Mann, M. Software lock mass by twodimensional
540 minimization of peptide mass errors. *J. Am. Soc. Mass Spectrom* **2011**, 22,
541 1373−1380.

542 (36) Luber, C. A.; Cox, J.; Lauterbach, H.; Fancke, B.; Selbach, M.; Tschopp, J.;
543 Akira, S.; Wiegand, M.; Hochrein, H.; O'Keeffe, M.; Mann, M. Quantitative
544 proteomics reveals subset-specific viral recognition in dendritic cells. *Immunity*
545 **2010**, 32, 279−289.
546 (37) Gene Ontology Consortium. The gene ontology (GO) database and informatics
547 resource. *Nucleic Acids Res.* **2004**, 32, 258−261.
548 (38) Ashburner, M., Ball, C.A., Blake, J.A., Botstein, D., Butler, H., Cherry, J.M.,
549 Davis, A.P., Dolinski, K., Dwight, S.S., Eppig, J.T., Harris, M.A., Hill, D.P.,
550 Tarver, L.I., Kasarskis, A., Lewis, S., Matese, J.C., Richardson, J.E., Ringwald, M.,
551 Rubin, G.M., Sherlock, G. Gene Ontology: tool for the unification of biology. *Nat.*
552 *Genet*. **2000**, 25, 25–29.
553 (39) Ahmad, I.; Cheng, Z. H.; Meng, H. W.; Liu, T. J.; Nan, W. C.; Khan, M. A.;
554 Wasila, H.; Khan, A. R. Effect of intercropped garlic (Allium sativum) on
555 chlorophyll contents, photosynthesis and antioxidant enzymes in pepper. *Pak. J.*
556 *Bot.* **2013**, 45, 1889−1896.
557 (40) Fan, H. T.; Song, B. A.; Bhadury, P. S.; Jin, L. H.; Hu, D. Y.; Yang, S. Antiviral
558 activity and mechanism of action of novel thiourea containing chiral phosphonate
559 on tobacco mosaic virus. *Int. J. Mol. Sci.* **2011**, 12, 4522−4535.
560 (41) Dietz, K. J.; Turkan, I.; Krieger-Liszkay, A. Redox- and Reactive Oxygen
561 Species-Dependent Signaling into and out of the Photosynthesizing Chloroplast.
562 *Plant Physiol.* **2016**, 171, 1541-1550.

563 (42) Thissen, D.; Steinberg, L.; Kuang, D. Quick and Easy Implementation of the
564 Benjamini-Hochberg Procedure for Controlling the False Positive Rate in Multiple
565 Comparisons. *J. Educ. Behav. Stat.* **2002**, 27, 77–83.
566 (43) Selinski, J.; Konig, N.; Wellmeyer, B.; Hanke, G. T.; Linke, V.; Neuhaus, H. E.;
567 Scheibe, R. The plastid-localized NAD-dependent malate dehydrogenase is crucial
568 for energy homeostasis in developing Arabidopsis thaliana seeds. *Mol. Plant* **2014**,
569 7, 170-186.
570 (44) Selinski, J.; Scheibe, R. Malate valves: old shuttles with new perspectives. *Plant*
571 *Biol.* **2019**, 1, 21-30.
572 (45) Scheibe, R. $NADP^+$-malate dehydrogenase in C3-plants: Regulation and role of a
573 light-activated enzyme. *Physiol. Plantarum* **1987**, 71, 393-400.
574 (46) Marri, L.; Pesaresi, A.; Valerio, C.; Lamba, D.; Pupillo, P.; Trost, P.; Sparla, F.
575 In vitro characterization of Arabidopsis CP12 isoforms reveals common
576 biochemical and molecular properties. *J. Plant Physiol*. **2010**, 167, 939-950.
577 (47) Arnér, E. S. J.; Holmgren, A. Physiological functions of thioredoxin and
578 thioredoxin reductase. *Eur. J. Biochem*. **2000**, 267, 6102-6109.
579 (48) Ifuku, K.; Endo, T.; Shikanai, T.; Aro, E. M. Structure of the chloroplast NADH
580 dehydrogenase-like complex: nomenclature for nuclear-encoded subunits. **2011**, 52,
581 1560-1568.
582 (49) Dietz, K. J.; Jacob, S.; Oelze, M. L.; Laxa, M. Tognetti, V.; Miranda, S. M. N.;
583 Baier, M.; Finkemeier, I. The function of peroxiredoxins in plant organelle redox
584 metabolism. *J Exp Bot*, **2006**, 57, 1697–1709.

585 (50) Yang, Y. F.; Shen, D. J.; Long, Y. J.; Xie, Z. X.; Zheng, H. Z. Intrinsic
586 Peroxidase-like Activity of Ficin. *Sci. Rep.* **2017**, 7, 43141-43148.

588 **Information of Figure**

589 Figure 1. Chemical structures of Ningnanmycin, Ribavirin, and Indole.

590 Figure 2. Design of target compounds.

591 Figure 3. Synthetic route for target compounds **D1-D25**.

592 Figure 4. Synthetic route for target compounds **D26-D28**.

593 Figure 5. Effects of compound **D21** on chlorophyll a (A), chlorophyll b (B) and
594 chlorophyll total (C), chlorophyll a/b (D) in tobacco leaves. Straight bars signify mean
595 ± SD (n = 3).

596 Figure 6. Effects of compound **D21** on superoxide dismutase (SOD, A), peroxidase
597 (POD, B), phenylalanine ammonia lyase (PAL, C), and catalase (CAT, D) activity in
598 tobacco leaves. Straight bars signify mean ± SD (n= 3).

599 Figure 7. Venn diagram shows that the proteome distribution between the **D21+PVY**
600 and **CK+PVY** groups changes uniquely and shares proteins.

601 Figure 8. Volcano plot of the relative protein abundance changes between the
602 **D21+PVY** and **CK+PVY** treatments. The red points show significantly up-regulated
603 proteins, whereas the blue points show significantly down-regulated proteins.

604 Figure 9. MDH signaling pathway in tobacco response to **D21**. Red color represents
605 the up-regulated proteins in this pathway. (Fd, Ferredoxin; FNR, ferredoxin-NADP
606 reductase; FTR, Ferredoxin-thioredoxin reductase; MDH, malate dehydrogenase;
607 NTRC, chloroplast NADPH-thioredoxin reductase; OAA, oxaloacetate; OMT,
608 malate/OAA translocators; PS Ⅰ, photosystem Ⅰ; PS Ⅱ, photosystem Ⅰ; ROS,
609 reactive oxygen species; Trx, thioredoxin).

610 Figure 10. **D21** effects on the NAD-MDH and NADP-MDH activities of tobacco

611 leaves at day 3. Straight bars signify mean ± SD (n= 3).

613 **Table 1. Antiviral Activity of the Target Compounds against PVY, CMV, and**
614 **TMV at 500 μg/mL[a]**

Compd.	R^1	R^2	X	Anti-PVY		Anti-CMV		Anti-TMV	
				curative effect (%)	protective effect (%)	curative effect (%)	protective effect (%)	curative effect (%)	protective effect (%)
D1	H	2-Hydroxyethyl	Cl	53.1±3.69	57.9±1.69	53.8±2.15	57.4±4.17	59.9±2.93	52.9±2.94
D2	H	Ethyl	Cl	55.7±3.44	60.1±3.56	60.3±3.03	60.1±3.80	59.5±3.91	55.2±3.23
D3	H	Propyl	Cl	52.8±1.20	53.1±1.95	59.7±3.87	57.8±4.37	60.4±3.07	58.4±3.90
D4	H	Isopropyl	Cl	32.0±3.33	31.7±3.50	25.2±0.58	33.6±3.03	44.4±1.66	25.9±3.22
D5	H	4-Chlorophenyl	Cl	57.4±1.87	56.7±3.02	60.6±4.13	54.3±3.71	61.1±3.34	53.3±4.45
D6	H	2,4-Dichlorophenyl	Cl	50.7±2.22	50.5±1.70	48.6±3.66	47.0±1.20	53.3±4.11	33.9±3.18
D7	H	Butyl	Cl	28.6±2.23	21.1±3.67	35.7±3.86	20.4±2.60	33.3±1.93	28.1±4.09
D8	H	Tert-buty	Cl	25.5±1.40	24.9±2.95	25.5±1.40	21.1±2.19	31.7±3.62	36.1±1.80
D9	H	Dodecyl	Br	50.2±2.73	47.7±1.29	60.2±3.65	57.3±3.30	51.6±2.70	56.9±3.28
D10	H	2-Hydroxyethyl	Br	52.9±2.39	49.1±3.74	50.8±2.10	57.7±2.52	56.7±2.62	65.1±3.67
D11	H	Ethyl	Br	51.0±2.05	45.2±3.30	57.9±2.80	59.2±3.13	50.6±1.91	62.0±2.49
D12	H	Propyl	Br	51.2±3.24	40.8±3.36	57.9±3.32	55.4±3.14	61.2±1.77	62.1±3.72
D13	H	Isopropyl	Br	33.6±1.62	32.9±2.52	34.5±2.50	36.8±1.28	40.3±4.15	39.3±1.40
D14	H	4-Chlorophenyl	Br	47.8±2.38	49.1±0.07	55.7±2.67	53.2±3.82	56.8±3.85	58.4±2.24
D15	H	2,4-Dichlorophenyl	Br	32.7±1.48	30.7±2.50	49.8±3.38	47.3±3.23	48.5±3.04	55.6±4.44
D16	H	Butyl	Br	27.9±3.73	45.8±1.65	32.4±3.61	29.6±2.66	33.4±3.17	44.0±4.73
D17	H	Tert-buty	Br	19.3±3.89	23.3±3.00	28.3±1.64	26.4±3.32	30.1±4.22	33.3±5.01
D18	H	Dodecyl	Br	45.1±1.96	55.2±4.35	53.5±2.65	52.4±3.43	54.6±3.36	52.7±4.97
D19	5-Br	2-Hydroxyethyl	Cl	35.0±1.08	35.5±3.60	60.8±3.57	55.3±3.52	56.3±3.94	64.3±3.53
D20	5-Br	4-Chlorophenyl	Cl	51.8±3.33	48.4±3.99	60.8±3.39	53.3±2.64	60.1±3.61	50.2±3.30
D21	5-Br	Propyl	Cl	61.6±2.49	70.1±1.45	61.1±2.39	63.2±3.16	59.7±3.46	63.1±3.39
D22	H	2-Hydroxyethyl	CH_3	50.0±2.40	55.1±2.39	54.5±2.36	50.2±1.46	57.5±2.76	59.1±3.79
D23	H	Ethyl	CH_3	55.5±3.17	57.8±3.73	53.2±4.19	51.1±1.71	58.4±3.97	60.1±4.73
D24	H	Propyl	CH_3	57.7±2.25	61.4±3.31	58.5±3.06	50.5±2.52	53.1±2.73	60.6±2.17
D25	H	4-Chlorophenyl	CH_3	55.7±3.40	55.3±1.63	44.1±3.97	46.1±3.14	58.6±3.84	58.7±4.38
D26	H	-	Cl	53.8±2.37	42.7±3.19	47.4±3.62	53.9±3.03	51.3±1.50	48.9±3.69
D27	H	-	Br	43.9±3.82	31.0±4.43	48.4±2.15	50.6±3.36	45±3.39	55.5±4.97
D28	5-Br	-	Cl	54.3±2.88	47.5±3.72	51.8±2.69	52.3±2.75	25.8±3.90	41.7±3.09
Ningnanmycin[b]	-	-	-	50.1±2.88	50.8±2.04	48.2±2.55	49.6±2.71	53.3±1.55	66.6±2.84
XCLSBM[c]	-	-	-	55.2±2.29	57.7±2.62	54.9±2.56	57.8±3.53	48.7±2.70	49.1±1.62
Ribavirin[d]	-	-	-	40.2±2.26	41.2±2.30	41.7±2.07	43.1±2.53	45.5±3.77	48.6±2.05

615 [a]Average of three replicates; [b]Ningnanmycin, [c]XCLSBM, and [d]Ribavirin were used as control, and
616 XCLSBM is lead compound Xiangcaoliusuobingmi.

617

618 **Table 2. EC_{50} Values of the Target Compounds against PVY, CMV, and TMV**
619 **(μg/mL)** [a]

Compd.	EC_{50} for PVY		EC_{50} for CMV		EC_{50} for TMV	
	Curative activity	Protective activity	Curative activity	Protective activity	Curative activity	Protective activity
D1	425±9.13	282±10.6	381±8.43	241±9.46	225±7.82	434±8.31
D2	285±9.32	212±7.81	199±6.47	187±8.95	255±8.14	366±6.24
D3	462±7.56	430±8.23	220±7.33	235±6.53	209±6.85	261±9.24
D4	1620±10.4	1760±6.37	-	1630±10.3	621±9.47	-
D5	272±7.77	365±9.88	202±7.83	356±7.37	215±8.57	428±6.46
D6	489±9.61	504±9.91	486±5.72	616±8.86	420±10.3	1570±9.78
D7	-	-	1470±8.67	-	-	-
D9	511±11.3	568±5.82	194±6.22	240±8.91	457±5.92	304±7.24
D10	434±6.97	484±6.55	438±7.13	223±5.73	322±9.24	207±6.73
D11	462±8.75	627±7.37	225±10.3	200±9.35	423±7.16	228±11.7
D12	507±6.72	821±8.42	224±6.48	297±5.92	220±9.17	216±7.65
D13	1450±9.48	1550±7.91	1550±8.85	1430±6.28	-	-
D14	552±10.4	503±7.86	284±8.43	285±5.23	364±5.66	273±9.53
D15	1540±5.91	1780±6.95	457±5.62	584±7.75	523±7.92	312±8.55
D16	-	618±4.18	1720±7.13	-	1650±8.47	723±7.75
D18	582±8.43	348±8.60	292±9.13	419±8.45	395±5.89	439±5.53
D19	1170±8.34	1090±5.72	217±6.95	313±6.76	342±8.82	212±8.12
D20	455±8.83	549±7.14	202±8.94	276±11.0	212±7.51	514±7.28
D21	217±9.96	122±7.86	179±5.38	156±8.87	209±6.45	200±10.1
D22	493±9.29	358±6.92	281±4.92	413±7.54	293±7.46	243±7.53
D23	313±7.86	268±9.84	293±6.54	386±6.46	293±10.4	250±8.22
D24	288±5.33	244±6.97	234±8.57	403±8.37	432±9.67	241±6.36
D25	302±10.3	362±10.1	673±9.38	592±9.66	241±6.42	238±9.93
D26	418±8.26	652±7.74	526±9.24	369±11.6	464±7.42	515±8.36
D27	632±9.69	1700±5.54	597±6.83	403±7.36	626±8.84	363±5.38
D28	399±10.6	558±6.26	373±9.44	362±9.33	-	-
Ningnanmycin[b]	468±4.67	464±8.52	498±6.47	439±7.45	382 ±6.13	198±10.7
XCLSBM[c]	292±7.48	279±7.67	275±6.94	240±6.77	517 ± 5.72	497±5.88
Ribavirin[d]	686±8.29	653 ± 5.83	704±9.45	690±5.38	668 ± 7.22	568±8.46

620 [a]Average of three replicates; [b]Ningnanmycin, [c]XCLSBM, and [d]Ribavirin were used as control, and
621 XCLSBM is lead compound Xiangcaoliusuobingmi.

622

623

624

625 **Table 3. DEPs involved in MDH pathway**

Protein ID	Protein Name	Length	Log Ratio	p-Value	Sig|Specific
A0A1S4BCV5_TOBAC	Malate dehydrogenase (EC 1.1.1.37)	220	3.29	1.26×10^{-2}	up
A0A1S4A5W5_TOBAC	Malate dehydrogenase (EC 1.1.1.37)	598	1.11	1.31×10^{-2}	up
A0A1S3X0Y5_TOBAC	Malate dehydrogenase (EC 1.1.1.37)	362	3.21	2.68×10^{-2}	up
A0A1S3X2I0_TOBAC	Malate dehydrogenase (EC 1.1.1.37)	174	2.68	3.61×10^{-3}	up
A0A1S4D2Y9_TOBAC	Malate dehydrogenase, glyoxysomal-like	215	1.58	4.48×10^{-2}	up
A0A1S3X756_TOBAC	Malic enzyme	199	3.28	2.11×10^{-2}	up
A0A1S4CY61_TOBAC	Thioredoxin	83	1.22	7.31×10^{-2}	up
A0A1S4B5N2_TOBAC	Thioredoxin	164	1.04	4.58×10^{-2}	up
A0A1S4C5L2_TOBAC	Thioredoxin Y1	143	5.27	2.65×10^{-2}	up
A0A1S4D4V1_TOBAC	Thioredoxin-like	164	1.08	4.81×10^{-2}	up
A0A1S3YXG6_TOBAC	Calvin cycle protein CP12-3, chloroplastic	341	10.0		up
A0A1S4BCB4_TOBAC	Ferredoxin	226	2.26	3.09×10^{-2}	up
A0A1S4D678_TOBAC	Ferredoxin-thioredoxin reductase, catalytic chain (EC 1.8.7.2)	229	3.48	2.27×10^{-2}	up
A0A1S4DK72_TOBAC	Ferredoxin-thioredoxin reductase, variable chain-like	162	1.62	4.10×10^{-2}	up
A0A1S3ZUX0_TOBAC	NADH dehydrogenase [ubiquinone] 1 alpha subcomplex subunit 2-like	123	1.13	1.77×10^{-2}	up
A0A1S4AA06_TOBAC	NADH dehydrogenase [ubiquinone] 1 alpha subcomplex subunit 8-B-like	118	3.87	1.40×10^{-3}	up
A0A1S4AQI3_TOBAC	NADH dehydrogenase [ubiquinone] 1 beta subcomplex subunit 7-like	184	2.31	8.49×10^{-3}	up
A0A1S4D700_TOBAC	NADH dehydrogenase [ubiquinone] iron-sulfur protein 5-B-like	186	10.0		up
A0A1S4C8V8_TOBAC	NADH dehydrogenase [ubiquinone] iron-sulfur protein 6	126	-10.0		down
A0A1S4CFV4_TOBAC	Peroxidase (EC 1.11.1.7)	93	10.0		up
D2K7Z2_TOBAC	Peroxiredoxin (EC 1.11.1.15)	168	1.95	2.58×10^{-2}	up
A0A1S4A969_TOBAC	Peroxiredoxin (EC 1.11.1.15)	234	1.80	1.02×10^{-2}	up
A0A1S3XK17_TOBAC	Peroxiredoxin (EC 1.11.1.15)	95	1.13	4.49×10^{-2}	up
A0A1S4CVN6_TOBAC	Peroxiredoxin (EC 1.11.1.15)	123	3.29	2.52×10^{-3}	up
A0A1S4DAA2_TOBAC	Peroxiredoxin (EC 1.11.1.15)	258	1.51	1.40×10^{-2}	up
A0A1S4AFD5_TOBAC	Photosystem I reaction center subunit IV B	180	1.07	9.33×10^{-3}	up

626